Journal Pre-proof

Long acting injectables for therapeutic proteins

Sally Ryan, Kim Shortall, Michele Dully, Ahmed Djehedar, David Murray, James Butler, John Neilan, Tewfik Soulimane, Sarah P. Hudson

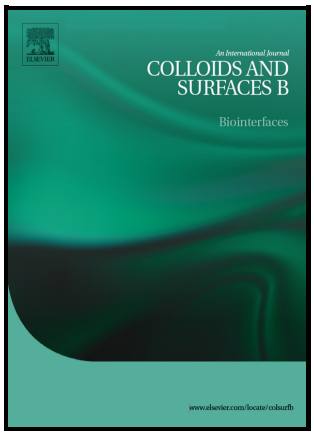

PII: S0927-7765(22)00327-7

DOI: https://doi.org/10.1016/j.colsurfb.2022.112644

Reference: COLSUB112644

To appear in: *Colloids and Surfaces B: Biointerfaces*

Received date: 18 March 2022
Revised date: 10 June 2022
Accepted date: 13 June 2022

Please cite this article as: Sally Ryan, Kim Shortall, Michele Dully, Ahmed Djehedar, David Murray, James Butler, John Neilan, Tewfik Soulimane and Sarah P. Hudson, Long acting injectables for therapeutic proteins, *Colloids and Surfaces B: Biointerfaces,* (2022) doi:https://doi.org/10.1016/j.colsurfb.2022.112644

Long acting injectables for therapeutic proteins

Sally Ryan[1], Kim Shortall[1], Michele Dully[1], Ahmed Djehedar[1], David Murray[2], James Butler[2], John Neilan[2], Tewfik Soulimane[1,*] and Sarah P. Hudson[1,*]

[1]Department of Chemical Sciences, CÚRAM, an SFI Research Centre Designing The Next Generation of 'Smart' Medical Devices, Bernal Institute, University of Limerick, Limerick, Ireland
[2]COOK Medical Ireland Limited, O'Halloran Rd, Castletroy, Limerick, Ireland
*Correspondence: Tewfik.soulimane@ul.ie and/or Sarah.hudson@ul.ie

Statistical Summary

Total Number of Words:	7577
Number of Figures:	4
Number of Tables:	4

Long acting injectables for therapeutic proteins

Sally Ryan[1], Kim Shortall[1], Michele Dully[1], Ahmed Djehedar[1], David Murray[2], James Butler[2], John Neilan[2], Tewfik Soulimane[1,*] and Sarah P. Hudson[1,*]

[1]Department of Chemical Sciences, CÚRAM, an SFI Research Centre Designing The Next Generation of 'Smart' Medical Devices, Bernal Institute, University of Limerick, Limerick, Ireland
[2]COOK Medical Ireland Limited, O'Halloran Rd, Castletroy, Limerick, Ireland
*Correspondence: Tewfik.soulimane@ul.ie and/or Sarah.hudson@ul.ie

Abstract

Biotherapeutic development presents a myriad of challenges in relation to delivery, in particular for protein therapeutics. Protein delivery is complicated due to hydrophilicity, size, rate of degradation *in vivo*, low permeation through biological barriers, pH and temperature sensitivity, as well as the need to conserve its quaternary structure to retain function. To preserve therapeutic levels *in vivo*, proteins require frequent administration due to their short half-lives. Formulation strategies combining proteins with lipid carriers for parenteral administration show

potential for improving bioavailability, while preserving protein activity and bypassing the mucosal barriers of the body. Encapsulating protein in long acting injectable delivery systems can improve therapeutic indices by prolonging and controlling protein release and reducing the need for repeat interventions. Two lyotropic crystal forming lipids, monoolein and phytantriol, have been formulated to produce lipidic cubic phases and assessed for their use as long acting protein eluting injectables. Three soluble proteins, cytochrome *c*, glyceraldehyde-3-phosphate dehydrogenase and aldehyde dehydrogenase and one membrane protein, cytochrome *c* oxidase, were incorporated into bulk cubic phase formulations of each lipid system to comparatively assess protein release kinetics. The activity of the soluble proteins was measured upon release from a phytantriol bulk cubic phase and phytantriol cubosomes, produced using a liquid precursor method.

Key words: lipid cubic phase; cubosomes; long acting injectables; proteins; drug delivery

1. Introduction

The expansion in biotherapeutics and biopharmaceuticals, such as protein therapies, has driven the development of delivery systems to support prolonged and controlled release of proteins *in vivo*. [1],[2],[3] Unlike small molecule drugs that are generally delivered orally, biotherapeutics have low bioavailability after oral administration and can be degraded in the alimentary canal.[4] For these reasons, biotherapeutics are primarily delivered parenterally. However, they tend to be unstable, thus requiring formulation strategies to prevent aggregation and prolong their half-life *in vivo.* The benefits of using long acting injectable formulations to encapsulate and deliver proteins can include improving protein stability, solubility and bioavailability through site specific delivery. Delivery systems frequently include formulation steps that require high temperature, large mechanical stresses or the use of solvents that are too harsh for proteins.[5] Therefore, there is an increasing need to design delivery systems that are more compatible with complex protein structures.

The simple organisational unit of biological membranes are lipids. Thus, inspired by their prevalence in the body, as well as their biodegradable, bioadhesive and biocompatible nature, lipids are ideal for protein delivery applications.[6] Lipids are

amphiphilic molecules that consist of a hydrophilic head group and an elongated, hydrophobic, hydrocarbon chain, that spontaneously self-assembles upon the introduction of solvents, as a result of intermolecular forces.[7] For certain lipids, this assembly allows for the protection of the non-polar chain, through the formation of a thermodynamically stable liquid crystalline phase, displaying long range order in three dimensions.[8] These systems of amphiphilic molecules in water are called lyotropic liquid crystal systems and can be categorised into mesophases based on the internal structures formed.[9] The three most common mesophases are the lamellar[8], hexagonal[10, 11] and cubic phases[12] which are produced by varying the lipid-to-water ratios during formulation. Since it was initially suggested that the structure of the lipid cubic phase (LCP) was similar to that of naturally occurring membranes, the LCP has been used for the crystallization of membrane proteins due to the stabilizing effect of the phase on incorporated proteins.[13],[14] This has led to significant structural analysis on proteins within the cubic phase in order to understand protein location and improve crystallisation.

The LCP displays the most complex spatial organization of all known lyotropic liquid crystals and owing to its stabilizing effect on proteins, it is an attractive system for protein delivery.[9] The formation of the LCP and the size of the aqueous nanochannels are dependent on the lipid used, water content and temperature of the phase, which in turn govern the surface-to-volume ratio. These physicochemical properties of the LCP control the loading of biomolecules within the phase as well as their subsequent release.[15]

The bulk LCP is a viscous gel when formed and has an intricate internal structure consisting of a curved bicontinuous lipid bilayer that separates two networks of aqueous nano-channels that allows controlled release of molecules of varying physiochemical characteristics.[6],[16] The release mechanism from cubic phase gels are generally consistent in the literature, with most hydrophilic molecules incorporated following diffusion controlled release, at a rate consistent with Higuchis square root of time release kinetics and hydrophobic molecules requiring degradation of the phase for release following Korsmeyers-Peppas first-order kinetics.[17],[18] The diffusion constant, solubility and the partition coefficient of incorporated molecules all influence the rate of release from the phase while the geometry, porosity and degradation rate of the phase also play influential

roles.[19],[20] Several strategies have been employed in order to achieve controlled release of drugs and proteins from the LCP including the addition of cationic surfactants,[21] anionic phospholipids,[22] lipase inhibitors to prevent enzyme degradation of the phase[19] and selective alkylation of varying chain lengths to drugs in order to increase association with the lipid bilayer.[23] The LCP can encapsulate hydrophilic proteins, that will reside close to the emulsifier polar head or within the aqueous nanochannels, as well as lipophilic proteins, that will inhabit the lipid bilayer.[23] The most commonly explored lipids to formulate the LCP for protein encapsulation are monoolein (MO)[5],[24],[17],[25],[26] and phytantriol (PHYT)[12],[26],[27],[28]. The range of proteins of varying sizes that have previously been encapsulated in the LCP are summarised in Table 1. These proteins have been encapsulated in an LCP in order to either assess the impact that protein incorporation has on the phase, or to evaluate protein release profiles from the phase for long acting formulation strategies. No further analysis has been carried out to determine activity of said proteins after release from the LCP.

Table 1: List of proteins encapsulated in bulk cubic phase formulations arranged in order of increasing molecular weight (MW), including PDB accession numbers where available, lipid used, release duration and mesophase formed.

Protein	PDB	MW (kDa)	Lipid	Release duration (days)	Release media	Mesophase	Reference
Cytochrome c	1HRC	11.7	MO	22.5	PBS	Im3m	[24]
Lysozyme	1BWI	14.4	MO	21.1	PBS	Im3m	[24]
Lysozyme	1BWI	14.4	MO	*	*	Im3m	[25]
Brain-derived neurotrophic factor	1B8M	13.5	MO	*	*	Pn3m, Ia3d	[29]
Myoglobin	1YMB	15.3	MO	16	PBS	Im3m	[24]
T. lanuginosus lipase		29.6	PHYT	*	*	Pn3m	[28]
Ovalbumin	1OVA	42.7	MO	21.8	PBS	Im3m	[24]
FITC-Ova	1OVA	45.7	MO	16	PBS	Pn3m, H_{II}	[26]
FITC-Ova	1OVA	45.7	PHYT	16	PBS	Pn3m	[26]
Bovine haemoglobin	2QSP	64.5	MO	6	PBS	Pn3m, Ia3d	[17]

Conalbumin	1AIV	75.8	MO	17.9	PBS	Im3m	[24]
Transferrin	3QYT	76.8	MO	*	PBS	Pn3m	[5]
Ceruloplasmin	2J5W	122.3	MO	*	PBS	Pn3m, Ia3d	[30]
Glucose Oxidase	1CF3, 1GAL	160	MO	*	PBS	Pn3m, Ia3d	[30]
Apo-ferritin	1MFR	496.1	MO	17.8	PBS	Im3m	[24]

Abbreviations: HII – hexagonal phase, Im3m, Pn3m, Ia3d – cubic phase space group. "*" – indicates the study did not include release data but encapsulated proteins for analysis of phase formation.

Within the cubic phase, a range of cubic space groups can be formed, either, body-centred, Ia3d and Im3m, or primitive lattice, Pn3m.[31] All three cubic space groups have been formulated to encapsulate proteins, Table 1. The smallest and largest proteins encapsulated in the cubic phase, cytochrome c, an 11.7 kDa protein of approximately 3.3 nm in diameter and apo-ferritin, a 496.1 kDa protein of approximately 12.6 nm in diameter, are both soluble and therefore should release from the LCP by diffusion. Results reported release of these proteins from the MO cubic phase for extended periods of ~ 23 and ~17 days respectively *in vitro*. However, the percentage release recorded for cytochrome c was between 70-80 % whereas for apoferritin release was less than 12%. The difference in the amount of protein released was attributed the ease of diffusion from the phase for smaller proteins through the aqueous nanochannels while larger proteins are trapped in the phase.[24] However, from the release profiles demonstrated by other proteins in Table 1 it is clear that release is not governed by size alone. Several of the other proteins have release profiles ranging between 6 and 21 days in release duration, with varying percentage releases. For example, bovine haemoglobin and conalbumin, with similar sizes of 64.5 kDa and 74.8 kDa had drastically different release profiles. Bovine haemoglobin was release at two temperatures 25 °C and 37 °C with cumulative release of 52% and 41% respectively in one day. Conversely, conalbumin was released over a 3 week period and only 12 % cumulative release was observed. To compare protein release between lipid systems from MO and PHYT cubic phases, a 45.7 kDa protein, fluorescently labelled ovalbumin (FITC-Ova) was encapsulated.[26] Release of FITC-Ova from both systems was prolonged however PHYT matrices, which remained in the cubic phase, exhibited a higher release (~30%) over shorter timeframes than the MO matrices (~10%), which underwent a phase transition from the cubic (Pn3m) to the hexagonal (H_{II}) phase.[26]

It appeared that the hexagonal phase slowed down the release from the MO matrix. These comparisons demonstrate that the physiochemical characteristics of both the matrix including phase and composition as well as the protein characteristics all have an impact on release rates. Overall, the percentage release observed for larger proteins has been accredited to the flexibility of the liquid crystal system facilitating molecular breathing or peristalsis creating transient sections of water channels large enough for larger proteins to pass through.[24] Angelova and co-workers have also noted the successful incorporation of large proteins in the relatively smaller channels of lipid cubic systems, attributing their incorporation to the presence of spacious nano-pockets within the cubic structures, [5, 15, 48] The prolonged protein release durations observed highlight the suitability of the LCP for controlled protein release considering the drastic size difference between these proteins and the ~ 5 nm diameter of the hydrated aqueous channels in the MO cubic phase.[15]

One disadvantage of using the LCP for injectable formulations is its characteristically high viscosity. Therefore, reducing viscosity to allow for ease of injection would be beneficial. One method of preserving the properties of the cubic phase while reducing viscosity is the dispersion of the phase into nanostructures called cubosomes.[31] Reduced viscosity would facilitate injection making cubosomes an appropriate carrier for local delivery of therapeutics. Cubosomes also have added benefits as delivery systems for applications such as solid tumour delivery, due to their nanoparticulate nature that facilitates the enhanced permeability and retention (EPR) effect which causes nanoparticles to accumulate within solid tumours.[33],[34] Cubosomes are also mucoadhesive which has driven research into their use for nasal[35] and ocular[36] therapeutic delivery to enhance therapeutic uptake across mucosal barriers. The mechanism of intracellular uptake of cubosomes and their interactions with cells is not entirely understood but is hypothesised to involve adsorption of cubosomes to cells, lipid exchange between the cubosome and the cell membrane and endocytosis by either receptor-mediated endocytosis or a non-specific uptake process called micropinocytosis.[37, 38] Several studies have demonstrated that the use of cubosomes can increase the concentration of the encapsulated molecules intracellularly, particularly in epithelial cells [39] and in delivery of active compounds to breast cancer cell lines.[40] Another recent study compared MO and PHYT cubosomes for intracellular delivery in cancer cells and

found PHYT cubosomes were better suited to crossing the cell membrane and delivering encapsulated molecules intracellularly in comparison to MO cubosomes and concluded that PHYT cubosomes used at low concentrations are nontoxic and efficient vehicles for therapeutic delivery to cancer cells.[41]

The most common method of cubosome preparation involves the mechanical dispersion of the preformed viscous cubic phase.[42] However, the energy required to disperse the cubic phase into submicron-sized cubosomes could impact the structure of the incorporated proteins.[5, 43, 44] An alternative method involves the use of a hydrotrope to dissolve the viscous liquid crystalline phase and induce a nucleation process upon subsequent dispersion in excess water with the optional addition of stabilisers. This results in the formation of cubic phase nanoparticles and the process is called the liquid precursor or solvent dilution method.[27],[45],[46] These methods form cubosomes with size ranges from 10 to 500 nm with water channel dimensions of 5–10 nm presenting a delivery system with similar applications to the bulk cubic phase but with enhanced injectability due to their reduced viscosity.

Stabilizers are required to prevent aggregation of cubosomes over time. However, the choice of stabilizer can impact the cubosome structure. Commonly used stabilizers include, Pluronic® F-127 [45], octyl glucoside, [48] and more recently Tween [46]. For example, cubic phases formulated with Tween 80 have demonstrated higher lattice parameters in comparison to cubosomes prepared with Pluronic F127.[46] Although cubosomes show promise as protein delivery vehicles, no FDA-approved cubosome formulations are on the market as of yet. However studies have increasingly been conducted comparing efficacy of FDA-approved drugs both alone and encapsulated in cubosome formulations, as demonstrated with Fungizone and Adriamycin.[47] Therefore it may be a matter of finding an application more suitable for cubosomes that would make them worthwhile compared to using a marketed nano-formulation for delivery. Several proteins have previously been encapsulated in cubosomes, Table 2.

Table 2: List of proteins encapsulated in cubosome formulations arranged in order of increasing molecular weight. Table includes PDB accession numbers, S – stabilizer used, H – hydrotrope used, lipid used, release duration in days, release media and mesophase formed (

Im3m, Pn3m, Ia3d – cubic phase space group). "–" - indicates a hydrotrope was not included in the formulation. "*" – indicates the study did not include release data.

Protein	PDB	MW (kDa)	Lipid	S	H	Release duration (days)	Release media	Phase	Reference
FITC-EFE	-	30.2	MO	F127	PG	1	PBS	Pn3m to Im3m	[48]
FITC-Ova	1OVA	45.7	MO	F127	PG	10	PBS	Pn3m, H_{II}	[27]
FITC-Ova	1OVA	45.7	PHYT	F127	PG	4	PBS	Pn3m	[27]
Fab frag - IgG1	1ACY	50.7	MO	OG	-	*	*	Pn3m, Im3m	[49]
Transferrin	1JNF	76.8	MO	OG	-	*	*	Pn3m, Im3m	[49]
IgG	1IGT	148.9	MO	OG	-	*	*	Pn3m, Im3m	[49]
Catalase	1QQW	239.0	MO	*	$TPEG_{1000}$	1	H_2O	Im3m	[50]
Fibrinogen	1DEQ	560.54	MO	OG	-	*	*	Pn3m, Im3m	[49]

Abbreviations: FITC- Fluorescein isothiocyanate, Ova- Ovalbumin, EFE - earthworm fibrinolytic enzyme, "frag" - fragment, IgG – immunoglobulin, MO – monoolein, PHYT – phytantriol, F127 - Pluronic® F-127, PG- Propylene glycol, OG - Octyl glucoside.

Of the proteins encapsulated into cubosomes, Table 2, only two were evaluated in terms of prolonged release, ovalbumin (FITC-Ova) and earthworm fibrinolytic enzyme (FITC-EFE), both fluorescently labelled with fluorescein isothiocyanate (FITC). The encapsulation of FITC-EFE using PHYT cubosomes was studied for delivery to the inner ear in an animal model. The results exhibited 2.6-fold higher concentrations of protein by analysis of cochlear fluid at each time point over a 24 hr study when compared with the same protein in solution.[48] The incorporation of FITC-Ova in both MO and PHYT cubosomes was achieved using the liquid precursor method and results indicated high protein entrapment as well as sustained release *in vitro*. However, in comparing both cubosome systems the authors observed longer release profiles for MO were due to conversion from the Pn3m cubic phase to the hexagonal (H_{II}) phase due to hydrolysis of MO to oleic acid.[27] Release of molecules from the hexagonal phase is much slower than the cubic

phase due to its' closed water channels as opposed to the open water channels in the cubic phase.[11] Due to the tendency for MO to phase transition, which could potentially impact release profiles, the authors concluded that PHYT cubosomes were more suitable for the preparation of cubosomes as therapeutic carriers.[27]

Prolonged release has been achieved for eight proteins from the bulk cubic phase and three proteins from cubosomes in the literature. Subsequent studies are required to further ascertain whether LCP formulations are appropriate for protein encapsulation, activity preservation and controlled release in long acting injectable formulations. In this work a selection of four model proteins were encapsulated into MO and PHYT bulk lipid cubic phases in order to probe the effect of protein physicochemical properties such as size, charge and solubility, on protein release profiles from bulk LCP. Furthermore, three soluble model proteins were incorporated into PHYT bulk and cubosome formulations to compare release profiles and protein activity upon release from the cubic phase with phase determination by SAXS analysis. Protein activity after release from both bulk and cubosome formulations was assessed to determine the suitability of the LCP and cubosomes for use as long-acting injectable protein delivery vehicles.

2. Materials and Methods

2.1 Materials

Commercial grade monoolein (1-(9Z-octadecenoyl)-rac-glycerol) (9.9 MAG) was received and used without further purification from Jena Biosciences. Phytantriol (3,7,11,15-tetramethyl-1,2,3-hexadecanetriol) was received and used without further purification from TCI (Tokyo Chemical Industry). Tween 80, propylene glycol, chloroform, cytochrome c from equine heart ≥ 95% purity, phosphate buffered saline (PBS) tablets, 2,2(-azino-bis(3-ethylbenzthiazoline-6-sulfonic acid) (ABTS) tablets, β-nicotinamide adenine dinucleotide (NAD^+), hexanal 98% and GAPDH Activity assay kit were received and used without further purification from Sigma-Aldrich. Hydrogen peroxide (30% w/v) was received and used without further purification from Mallinckrodt Chemicals. Water used throughout was purified using a Milli-Q Water System (Millipore Corporation, Bedford, MA) consisting of a carbon filter cartridge, two ion-exchange filter cartridges and an organic removal cartridge.

2.1 Recombinant protein production

Cytochrome C oxidase (CYT C OX), and aldehyde dehydrogenase (ALDH) were recombinantly produced as previously described.[59],[60]

2.2 Glyceraldehyde-3-phosphate dehydrogenase (GAPDH) recombinant production

The commercially available construct DNA for human GAPDH in plasmid pEZY19 was transformed into Escherichia coli BL21 Star (DE3) competent cells. The auto-induction ZYM-5052 medium, supplemented with ampicillin (100 µg/ml), was inoculated with an overnight culture of the transformed cells at 1% (v/v), and grown for 24 h at 37 °C with shaking at 200 rpm. Centrifugation, washing and cell lysis were carried out as previously described, using 50 mM Tris-HCl, 500mM NaCl pH 8 at 5 mL/g of biomass.[60] The supernatant was filtered through a 0.45 µm Sartorius™ Minisart™ Plus Syringe filter. A FastFLow Chelating Sepharose resin was charged with 200mM nickel (II) sulfate, and a stepped gradient imadazole dependant protein elution was carried out.[62] Concentration was carried out using Amicon Ultra-15 centrifugal filters (Merck Millipore) before loading onto a HiLoad 16/60 Superdex 200 pg column using 50 mM Tris-HCl, 50mM NaCl pH 7.6 buffer. Fractions containing protein were combined and concentrated. Protein purity was evaluated using SDS–PAGE on 12 % polyacrylamide gels and immunoblotting with monoclonal anti-polyhistidine-peroxidase antibody was used to confirm the presence of hexahistidine-tagged protein. Proteomic analysis was carried out in the Proteomics Facility, University of Aberdeen, Rowett Institute as previously described.[63]

2.3 Preparation of phytantriol and monoolein bulk cubic phase gels

Bulk cubic phase gels were prepared by heating 100mg of phytantriol or monoolein at 40°C until molten in glass vials. The aqueous content required to form the cubic phase based on the phase diagram for monoolein[64] and phytantriol[65], 40 % w/w and 30 % w/w respectively, was added directly into the molten lipid using a micropipette and the mixture was vortexed to mix. The samples were sealed and left to equilibrate in the dark at room temperature for at least 48 hours. Bulk cubic phase gels loaded with protein were prepared using the same method with the addition of protein included in the aqueous component. Protein encapsulation in phytantriol and monoolein cubic phase gels was 0.5 % w/w.

2.4 Preparation of phytantriol cubosomes

Cubosomes were prepared as previously described.[46] Briefly 100 mg phytantriol, Tween 80 (15% w/w) and co-solvent propylene glycol (70 % w/w) were combined in glass vials. Excess chloroform (≈10 mL) was added to the vials and evaporated in a vacuum oven at 45°C. 10 µL of water or aqueous protein solution (10 mg/mL), was added to the vials and briefly vortexed to mix. The samples were sealed and left to equilibrate in the dark overnight. The liquid precursor was then dispersed in 4 mL of PBS with vortexing for 5 min.

2.5 Release studies - phytantriol and monoolein bulk cubic phase gels

The release of entrapped protein from bulk cubic phase gels was monitored daily in PBS release media, at 37 °C and 200 rpm in a shaking incubator. 1 mL PBS was added into the glass vials containing the bulk cubic phase gels and at fixed time intervals the release media was completely removed and replaced with fresh release media. Release media was monitored for the presence of entrapped protein by UV-spectrophotometry and kinetic enzyme assays. Absorbance values obtained were analysed against standard curves. Release values were determined by calculating the difference between the total initial protein concentration and the released fraction of protein in the supernatant with results represented as cumulative percentage release. Each release study was performed in triplicate with sample sizes of $n > 3$.

2.6 Release studies - phytantriol cubosomes

Release studies of entrapped protein from phytantriol cubosomes were obtained by taking 200 µL aliquots of the dispersions at fixed time intervals. Samples were centrifuged for 30 min at 14,000 rpm to separate the cubosome fraction from the released protein fraction and the supernatant was analysed by UV-spectrophotometry and kinetic enzyme assays. Absorbance values obtained were analysed against standard curves. Release values were determined by calculating the difference between the total initial protein concentration and the free fraction of protein in the supernatant.

2.7 Enzyme activity assay - Cytochrome c

The enzymatic activity of cytochrome c release from phytantriol bulk cubic phase and cubosomes was assessed based on peroxidase activity using a chromogen, 2.2'-azinobis-(2-ethylbenzthiazoline-6-sulfonate) (ABTS) as previously described.[64] Briefly, cytochrome c catalysed the oxidation of the substrate ABTS by hydrogen

peroxide resulting in a time-dependent change in optical absorption spectra. Release media samples of 100 µL were assayed in a reaction mixture containing 10mM potassium phosphate buffer pH 7.4, 50µM ABTS and 0.3 mM hydrogen peroxide. Reduction in the absorbance of ABTS as a result of the formation of ABTS+ was monitored at 415nm. A substrate-lacking reaction was used as a negative control. One unit of enzyme was defined as the amount of enzyme which catalysed the formation of 1.0 µmol of ABTS+/min. All assays were performed as a minimum of three independent experiments with triplicates for each reaction.

2.8 Enzyme activity assay - GAPDH

The activity of recombinantly produced GAPDH released from the phytantriol bulk cubic phase and cubosomes was determined using a GAPDH activity assay kit. Release media samples of 100 µL were assayed in a reaction mixture based on the manufacturer's recommendations. The activity is determined in a coupled enzyme reaction in which glyceraldehyde-3-phosphate (GAP) is converted to 1,3-bisphosphate glycerate (BPG) by GAPDH through monitoring the formation of NADH at 450nm and comparing against a standard curve. 0, 2, 4, 6, 8 and 10 µL of 1.25 mM NADH standard was added into a series of wells containing the reaction buffer in a 96-well plate to generate 0, 2.5, 5.0, 7.5, 10 and 12.5 nmol/well NADH standard. The assay mixture was incubated at 37°C for 60 min, absorbance of each sample at 450 nm was measured at 0 min and 60 min, and GAPDH activity was calculated according to the absorbance values and NADH standard curve. One unit of GAPDH is the amount of enzyme that generated 1.0 µmole of NADH per minute at pH 7.2 at 37 °C. All assays were performed as a minimum of three independent experiments with triplicates for each reaction.

2.9 Enzyme activity assay – ALDH

The activity of recombinantly produced $ALDH_{530}$ from *Thermus thermophilus* was monitored spectrophotometrically by time dependant reduction of NAD^+ cofactor to NADH (λ excitation = 340 nm; λ emission = 463 nm). Release media samples of 100 µL were assayed in a reaction mixture containing 10 mM potassium phosphate buffer pH 8.0, 2 mM NAD^+ and 1 mM Hexanal at 50°C for 60 seconds to avoid evaporative loss of the volatile aldehydes. A substrate-lacking reaction was used as a negative control. One unit of enzyme was defined as the amount of enzyme that

catalysed the formation of 1.0 µmole of NADH/min. All assays were performed as a minimum of three independent experiments with triplicates for each reaction.

2.10 Polarised Light Microscopy (PLM)

The isotropic nature of the cubic phase means that polarised light is rotated within the mesophase producing dark images when samples are placed between crossed polarizers [65]. This method of visualisation was regularly employed for visual inspection of cubic phase samples at room temperature using a Zeiss AxioScope Optical microscope with polarized light filter and a cross-polarizer. Image acquisition was carried out using an AxioVision 4.8 imaging system by Carl Zeiss Ltd. Non-birefringence in refraction was identified by the appearance of a black image or zone on the camera.

2.11 Small-angle x-ray scattering (SAXS)

SAXS data collection was carried out at the Solution State SAXS B21 beam line at Diamond Light Source, UK as previously described.[19] The experiments were conducted at ambient temperature and a beam wavelength of λ = 13.1 keV. Beam size at the sample was approximately 1 mm × 1 mm with a flux of approximately 4×10^{12} photons per second delivered from the bending magnet source. 2D diffraction patterns were collected on an Eiger X 4 M detector that was configured to measure a scattering vector (q) range from 0.0032 to 0.38 $Å^{-1}$. Samples were subjected to 1 s X-ray exposure for a total of 15 frames at a constant location. Bulk samples were manually loaded into custom viscous sample holders for data collection.

2.12 Dynamic light scattering (DLS)

Particle size distribution (Z-average), polydispersity (PDI) and zeta potential of phytantriol dispersions were determined using photon correlation spectroscopy (PCS) (Malvern Zetasizer Nano ZSP system). The refractive indexes used for phytantriol and water were 1.48 and 1.33, respectively. Measurements were performed at 25 °C, and the results presented are the mean of three successive measurements of 100 s of at least three independent samples. The average value and the standard deviation between repeated measurements are reported. Samples were diluted with water to adjust the signal level.

3. Results

Two lipids, monoolein and phytantriol, were formulated to evaluate release profiles of proteins encapsulated in their bulk cubic phases. The release media used in this work, PBS, does not facilitate degradation of the lipid cubic phase and thus both MO and PHYT samples maintained a mesophase crystalline structure upon visual examination and using PLM before and after release studies. Therefore, due to the maintenance of the structural integrity of the formed gels, the release profiles are assumed to be controlled by diffusion of proteins from the cubic phase through the aqueous nanochannels into solution. For comparative purposes, four model proteins of varied size, both soluble and membrane associated, were encapsulated within the MO and PHYT bulk cubic phase: cytochrome c (CYT C), cytochrome c oxidase (CYT C OX), glyceraldehyde-3-phosphate dehydrogenase (GAPDH) and aldehyde dehydrogenase (ALDH). Figure 1(a) shows the cumulative release profiles for four model proteins from the bulk lipid cubic phase.

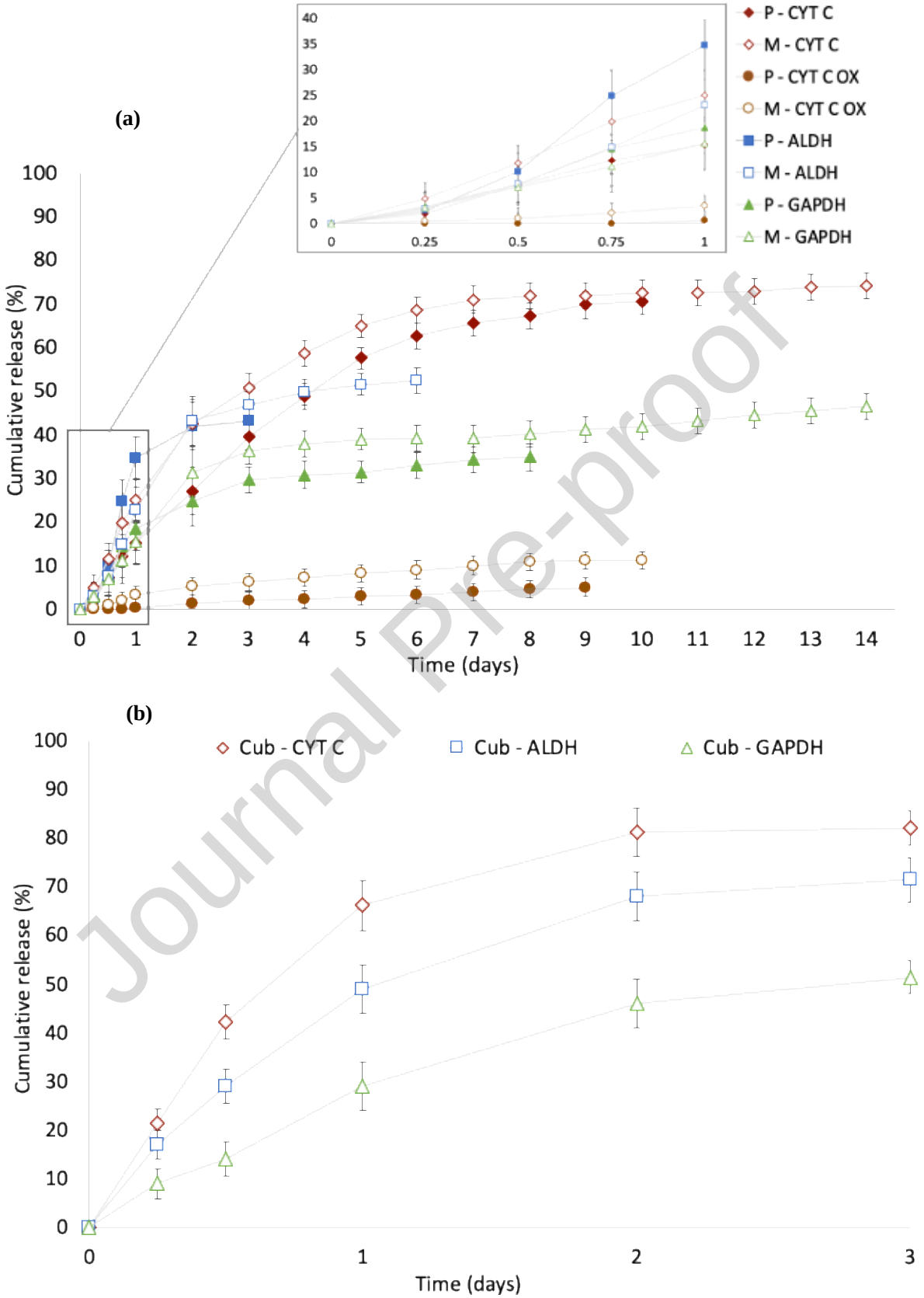

Figure 1: Cumulative release profiles for proteins from (a) the bulk lipid cubic phase P (phytantriol – closed symbols) and M- (monoolein- open symbols); Cytochrome c (CYT C; ◆),

Cytochrome c oxidase (CYT C OX; ●),Aldehyde dehydrogenase (ALDH; ■) and Glyceraldehyde-3-phosphate dehydrogenase (GAPDH; ▲) and (b) from phytantriol cubosomes; Cytochrome c (CYT C) (◊), Aldehyde dehydrogenase (ALDH) (□) and Glyceraldehyde-3-phosphate dehydrogenase (GAPDH) (△) released into PBS at 37 °C and 200 rpm in a shaking incubator. Release was monitored by UV-spectroscopy at represented timepoints until release was no longer detected.

The smallest of the incorporated soluble proteins, CYT C, a 12.3kDa protein, exhibited the highest cumulative release, 71% ± 3% and 74% ± 3% from PHYT and MO LCP bulk phases respectively. ALDH and GAPDH, much larger proteins than CYT C, exhibited a lower cumulative release. The cumulative release observed for ALDH, a 234.2 kDa protein, was 43% ± 4% in PHYT and 52% ± 3% from MO. This is higher in both lipid systems than that of GAPDH, a smaller, soluble protein (146.4 kDa), that demonstrated a cumulative release of 35% ± 4% from PHYT and 47% ± 4% from MO.

PHYT was examined further for development into a cubosome protein delivery system as the inability for enzymes such as esterases to degrade PHYT *in vivo* makes it a promising candidate for injection of therapeutic proteins in a prolonged release delivery system. The three model soluble proteins were incorporated into PHYT cubosomes to assess release profiles compared to bulk LCP release profiles. All three soluble proteins, CYT C, ALDH and GAPDH demonstrated increased cumulative protein release from cubosomes, Figure 1(b), compared to from bulk cubic phase, Figure 1(a). Release was complete over a shorter timeframe from the PHYT cubosomes for CYT C and GAPDH than from the bulk LCP, over 3 days compared to 8 and 10 days respectively. Meanwhile ALDH showed a similar rate of release, with maximum release from both bulk LCP and cubosome formulations reached in 3 days. The trend observed in the bulk cubic phase with the release of the smallest protein, CYT C, the fastest and to the highest extent was maintained by PHYT cubosomes.

The cubic phase in the PHYT bulk and cubosome samples, with and without proteins, were compared by structural analysis of the formed phase using phase determination by small angle X-ray scattering (SAXS) analysis, Table 3. SAXS analysis of the bulk PHYT cubic phase, confirmed the formation of the PHYT cubic

phase with the presence of two cubic mesophases coinciding concurrently, the Pn3m and the Ia3d cubic phases. These mesophases were detected both in the blank PHYT cubic phase as well as in the presence of encapsulated proteins CYTC, GAPDH and ALDH. The presence of CYT C, GAPDH and ALDH at 0.5% w/w had little impact on the lattice parameters. The observed two-phase region, Pn3m and Ia3d, has previously been described to exist in equilibrium in PHYT cubic phases with lattice parameters of 63.6 Å for Pn3m and 100.9 Å for Ia3d at 22 °C.[63] To assess the relationship between coexisting phases, Bonnet transformations can be calculated to determine the ratio between lattice parameters.[77] The theoretical calculation of the Bonnet ratio for Ia3d to Pn3m surface, without change in curvature is 1.57.[78] The calculated Bonnet ratio for the bulk cubic phase with ALDH incorporated was 1.57 and 1.55 for formulations including CYT C, GAPDH and blank cubic phases.

The formulation of PHYT cubosomes for the encapsulation of proteins was achieved using methods previously described and results obtained for average sizes (nm) and PDI were in agreement with those previously obtained for blank cubosomes.[46] Average blank PHYT cubosomes sizes were 224 nm ± 9 nm with no significant difference in particle sizes upon the incorporation of CYT C, GAPDH OR ALDH ($p < 0.05$), Table 3. The PDI of all cubosomes dispersions were less than 0.3, indicating unimodal distribution in particle size, which highlights the efficiency of the liquid precursor method in generating particles of uniform distribution.[27]

Table 3: PHYT bulk cubic phase (B) and cubosome (C) structural analysis: SAXS phase identification and lattice parameters of assigned mesophases with estimated dimensional values for water channel diameter (D) without protein encapsulation (blank) and with encapsulated proteins CYT C, GAPDH, and ALDH. LP – lattice parameter in angstrom (Å), BR – Bonnet ratio, Average nanoparticle size (nm), polydispersity index (PDI) and zeta potential (ZP), (mV) data presented represent the mean ± SD of three independent experiments of freshly prepared samples characterised upon dispersion in water. * - LP and D not available for these samples.

	Phase	LP (Å)	D (nm)	BR	Size (nm)	PDI	ZP (mV)
B - blank	Pn3m, Ia3d	70.4, 108.9	2.92	1.55	-	-	-
B - CYT C	Pn3m, Ia3d	70.1, 108.4	2.90	1.55	-	-	-

B - ALDH	Pn3m, Ia3d	68.6, 109.2	2.84	1.57	-	-	-
B - GAPDH	Pn3m, Ia3d	70.0, 108.8	2.89	1.55	-	-	-
C - blank	Pn3m	110.3	4.6	-	223.7 ± 9.2	0.2 ± 0.02	-25.1 ± 2.1
C - CYT C	Pn3m	*	*	-	225.6 ± 13.4	0.2 ± 0.02	-11.9 ± 3.0
C - ALDH	Pn3m	115.6	4.8	-	229.5 ± 11.8	0.2 ± 0.03	-32.7 ± 2.7
C - GAPDH	Pn3m	115.4	4.8	-	218.3 ± 10.6	0.2 ± 0.03	-10.6 ± 2.6

To evaluate the impact of incorporation into and release from the PHYT cubic phase, enzyme activity in the release media was monitored over time and compared against fresh protein activity in solution. The specific activities of free CYT C, GAPDH and ALDH in PBS were determined to be 6.4 U/mg ± 0.16, 34.7 U/mg ± 0.68 and 0.91 U/mg ± 0.03 respectively. Complete loss of activity was observed for the free proteins after 1 day for ALDH, 2 days for CYT C and 4 days for GAPDH when kept in PBS at 37°C with shaking, Figure 2.

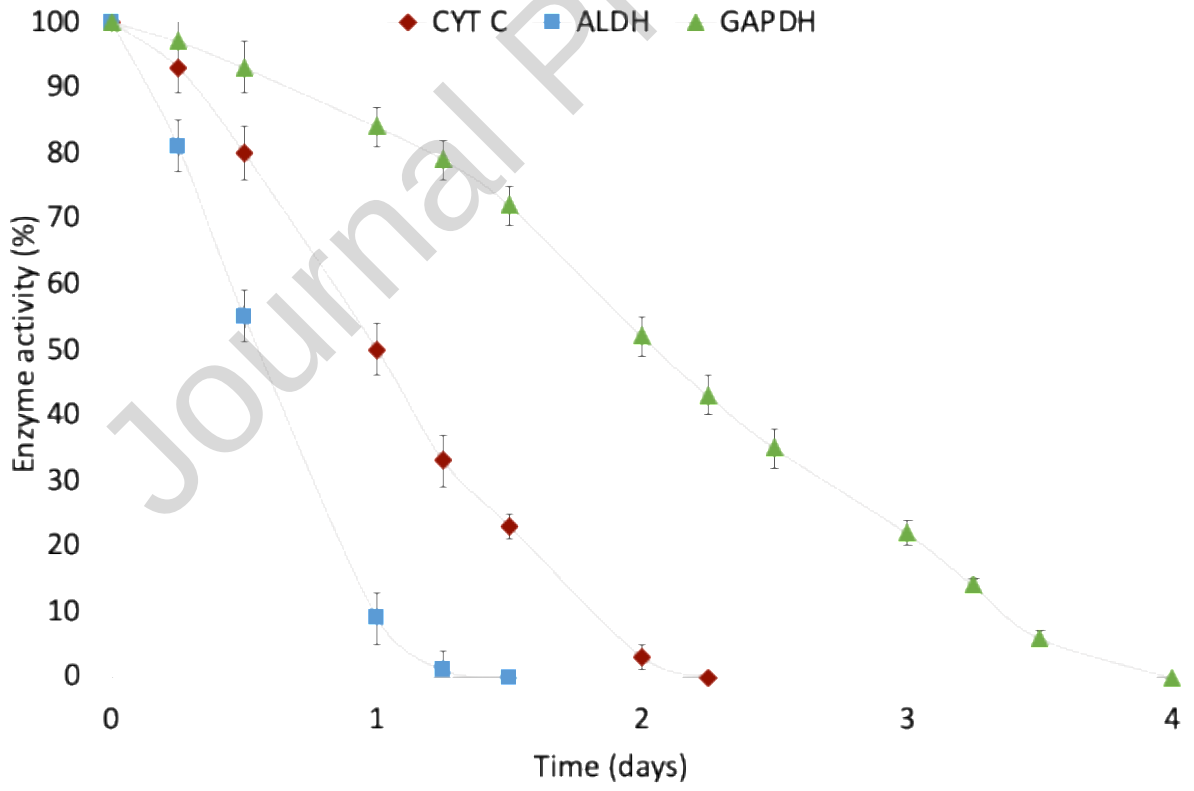

Figure 2: Activity of unencapsulated protein monitored over time in PBS at 37 °C and 200 rpm in a shaking incubator expressed as a percentage of initial activity CYT C (◆), ALDH (■ and GAPDH (▲).

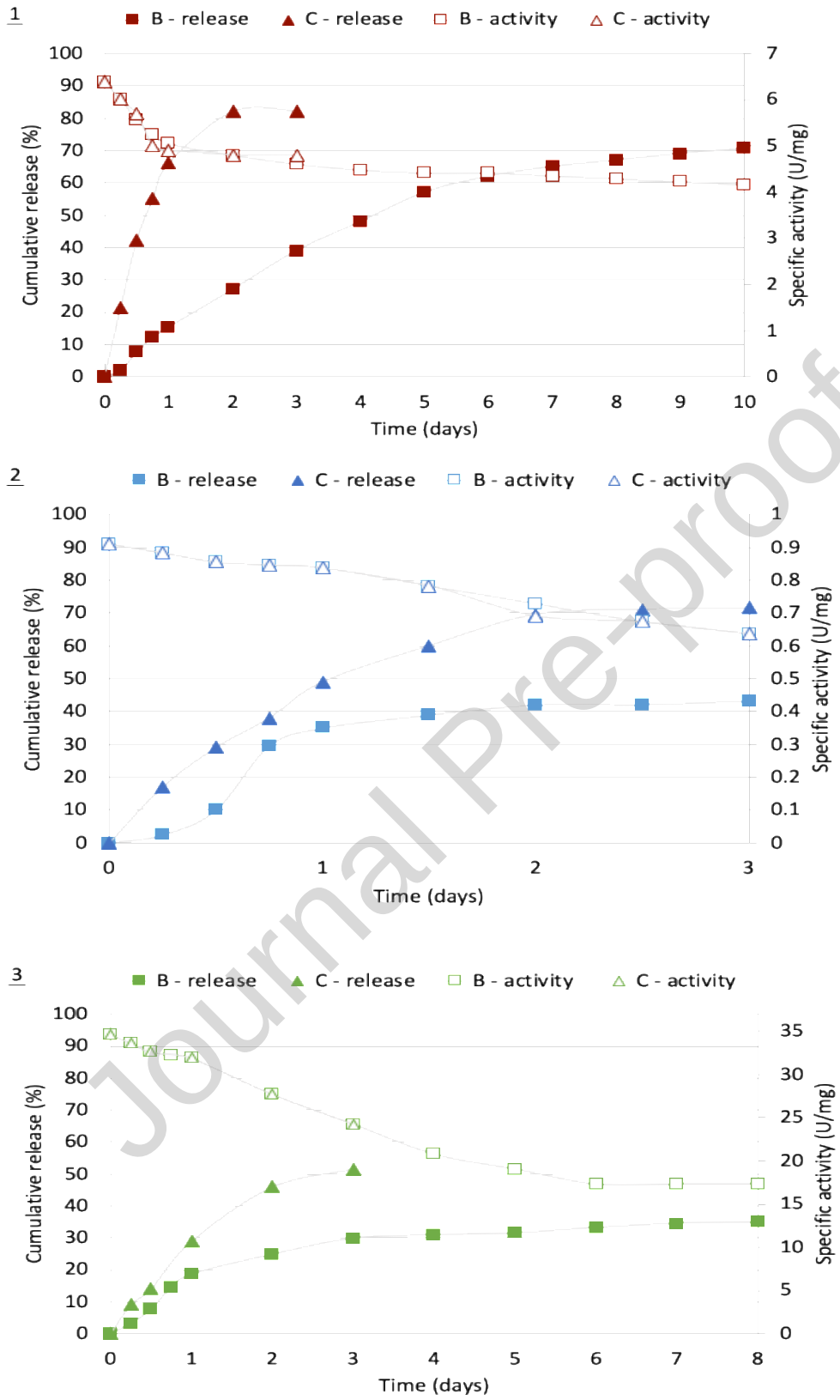

Figure 3: Release and activity of three proteins 1: CYT C, 2: ALDH and 3: GAPDH. from the lipid cubic phase in PBS at 37 °C and 200 rpm in a shaking incubator. Cumulative protein release (closed symbols) and specific activity (open symbols) were monitored from PHYT bulk (B) cubic phase (■) and cubosome (C) formulations (▲). Release and activity were monitored

by UV- spectrometry and enzyme assays at each represented timepoint until no further release was detected.

Stabilisation and extended protein activity were observed in all three proteins encapsulated within the PHYT cubic phase, Figure 3. Release and activity were monitored by UV-spectrometry and enzyme assays at each represented timepoint until no further activity or release was detected. Figure 3 demonstrates that release was observed to decrease slowly over time while the specific activity demonstrates that the protein activity is maintained by encapsulation in the lipid. Complete loss of activity was observed after 2 days for free CYT C in solution compared to a 40% ± 3% reduction in activity over 10 days from the bulk PHYT cubic phase and 35% ± 3% over 3 days in cubosome formulations. Similarly, free GAPDH activity was undetectable in solution after 4 days (and a 75% reduction in activity after 3 days) but GAPDH maintained activity for 8 days after release from the bulk cubic phase with a 50% ± 3% reduction in specific activity and a 30% ± 1% reduction in specific activity over three days in cubosomes. ALDH in solution was the fastest protein to degrade with complete loss of activity after 1 day, compared with sustained activity for 3 days when released from the bulk cubic phase and cubosomes with a 30% ± 3% and 31% ± 3% reduction in specific activity respectively.

4. Discussion

The development of long-acting injectable formulations for the delivery of proteins requires a system that exhibits enhanced protein stability to maintain function, increases protein half-life time *in vivo* and facilitates intracellular delivery. The main difference in the chosen cubic phase forming lipids, MO and PHYT, is their rate of degradation *in vivo.* Polar monoacylglycerols, such as monoolein, are composed of glycerol molecules linked to a fatty acid via an ester bond.[66] The contrast in stability in digestive environments between MO and PHYT is due to the presence of the ester linkage in the backbone of MO, that results in the digestion of the lipid by esterases as well as chemical instability at low and high pH.[23],[67] In this work protein release rates and activity upon release were monitored to compare the suitability of these systems for use as protein delivery vehicles. Both MO and PHYT were used to encapsulate four model proteins. Figure 4 demonstrates the structural

differences and relative sizes of the four model proteins, generated in Pymol (DeLano Scientific, South San Francisco, CA), using Protein Data Bank accession numbers 1OCD, 1EHK, 1U8F and 6FK3. The properties of each model protein are summarised in Table 4.

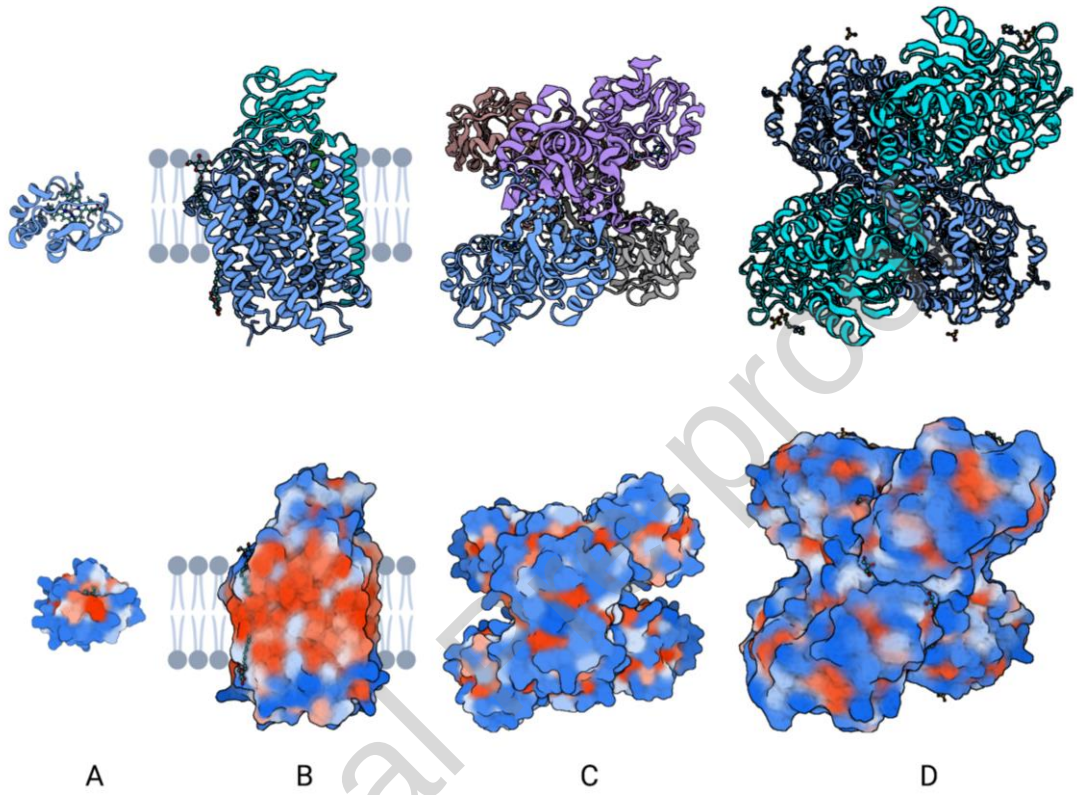

Figure 4: Four model proteins (A-D) A - Cytochrome c (PDB ID: 1OCD), B - Cytochrome c oxidase (PDB ID: 1EHK), C - Glyceraldehyde-3-phosphate dehydrogenase (PDB ID: 1U8F) and D -Aldehyde dehydrogenase (PDB ID: 6FK3). Top row: Figures were generated using Biorender with dimensions reproduced from measurements made in Pymol (DeLano Scientific, South San Francisco, CA). Bottom row: Electrostatic surface charge distribution of the four model proteins (A-D). Figures were generated using electrostatic charge distribution values calculated with APBS and PDB2PQR software where colours indicate electronegative charge -5 kT/e (red) to electropositive charge 5 kT/e (blue) on the protein surface.[73]

Table 4: Physiochemical properties of four model proteins. Dimensions represented were generated using the measurement wizard in Pymol (DeLano Scientific, South San Francisco, CA). PDB accession numbers, Isoelectric point and grand average of hydropathicity index (GRAVY) are also included for each protein.

	MW	PDB ID	Isoelectric	Dimensions (l x w x h)	GRAVY

	(kDa)		point (pI)	(nm^3)	
CYT C	12.3	1OCD	9.6	3.3 x 3.2 x 2.9	-0.9
CYT C OX	87.4	1EHK	9.0	5.4 x 4.9 x 7.8	0.7
GAPDH	146.4	1U8F	8.6	8.2 x 7.9 x 6.9	-0.1
ALDH	234.2	6FK3	6.1	9.8 x 9.5 x 8.0	-0.2

Abbreviations: MW - molecular weight, CYT C - Cytochrome c, CYTC OX - Cytochrome c oxidase, GAPDH - Glyceraldehyde-3-phosphate dehydrogenase and ALDH - Aldehyde dehydrogenase.

Three of the model proteins are water soluble and one, CYT C OX, is a membrane protein. The grand average of hydropathicity index (GRAVY) is included to represent the hydrophobicity value of each protein, which is generated by calculating the sum of the amino acids hydropathy values divided by the sequence length.[68],[69] Positive GRAVY values indicate hydrophobic proteins and negative values indicate hydrophilic proteins. This information indicates the potential location of the proteins within the cubic phase. Hydrophilic proteins will reside in the aqueous nanochannels, and hydrophobic proteins will be incorporated in the lipid bilayer. The computed isoelectric points of each protein calculated based on their amino acid sequences are included to contextualise protein charge in relation to the release media PBS.[69],[70],[71] Further analysis of protein charge was carried out using electrostatic charge distribution values calculated with APBS and PDB2PQR software[72], [73] represented also in Figure 4.

Overall, the cumulative release of the three soluble proteins, CYT C, ALDH and GAPDH, was much higher than the cumulative release of the membrane protein CYT C OX from both MO and PHYT LCPs, Figure 1. This is most likely due to the entrapment of CYT C OX within the lipid bilayer, thus requiring the degradation of the phase for protein release into solution, which is not facilitated in PBS. It is important to consider that membrane proteins, such as CYT C OX have large areas of hydrophobic regions that enable their localisation with lipid bilayers *in vivo.* Therefore, CYT C OX is more stable in the hydrophobic region of the cubic phase with low solubility in aqueous media hampering its release. Thus, hydrophobic proteins incorporated in the LCP preferentially reside within the lipid bilayers as opposed to in the aqueous water channels, making their subsequent release into an aqueous external environment much slower than hydrophilic proteins. These results further support the hypothesis that the release of hydrophobic molecules incorporated in the

LCP is dependent on the breakdown of the phase rather than diffusion from the phase.

The percentage release observed for soluble proteins, Figure 1, is interesting considering their large dimensions, Table 1, compared to the water channel dimensions of MO and PHYT cubic phases at 3-4nm [74],[49],[24] and 2-3 nm [75],[76] respectively. This has also been demonstrated in previous studies and is accredited to the flexibility of the liquid crystal system facilitating molecular breathing or peristalsis creating transient sections of water channels large enough for proteins to pass through.[24] Comparing protein release observed between soluble proteins, the protein size, isoelectric point and surface charge all appear to have an impact on the observed release rate. Although the cumulative release percentages observed follow similar trends for MO and PHYT, the timeframes for release of each incorporated protein are longer in MO compared to PHYT, Figure 1. Release studies showed the fastest protein release was for the smallest soluble protein (CYTC C), however if size is the primary factor impacting release then GAPDH should have followed and subsequently ALDH, however this was not the case. The faster release observed for ALDH may be attributed to its isoelectric point and distribution of surface charge. ALDH has an isoelectric point of 6.1, resulting in an overall negative charge in PBS compared to GAPDH, with an isoelectric point of 8.6 which is positively charged in PBS. The MO and PHYT polar head groups consist of hydroxyl groups that will have electrostatic interactions with positively charge regions on the proteins incorporated. GAPDH will have more affinity to the polar headgroups of the lipid bilayer compared to ALDH and these increased interactions will delay diffusion through the water channels. Conversely negatively charged proteins, such as ALDH, will not interact with the polar lipid head groups to the same extent. The isoelectric point gives an average of the overall surface charge of the protein but with these large protein molecules, concentrated electronegative and electropositive regions on the protein surface can interact independently. Increased interactions within the cubic phase have been reported in previous studies where increased hydrogen bonding identified by FTIR upon incorporation of a soluble protein, bovine haemoglobin, into MO cubic phases suggests that some transient interactions may be at play between lipids and proteins within the cubic phase.[17] These results

demonstrate the ability of the MO and PHYT bulk cubic phases to encapsulate and release incorporated proteins of varied sizes, surface properties and solubilities.
Another aspect of interest when considering the addition of soluble proteins with large dimensions to the cubic phase is the diameter of the aqueous channels (D). The blank PHYT cubic phase had a water channel diameter of 2.9 nm and encapsulation of CYT C, GAPDH and ALDH did not alter this dimension with diameters of 2.9 nm, 2.9 nm and 2.8 nm recorded respectively, Table 3. This is consistent with previous studies that noted minute changes to space groups and lattice parameters regardless of the incorporation of large proteins into the phase.[5],[28] However, protein concentrations of 10 wt.% have previously demonstrated phase transitions.[28] In this case, protein concentrations of 0.5% w/w were used as the catalytic nature of the incorporated proteins allows for high activities at low loadings, unlike the high loading that would be required for long acting injectable antibody therapeutics which act in a stoichiometric fashion with their biological targets.

Previously described formulation methods for the production of PHYT cubosomes using the liquid precursor method provide a suitable approach for protein loaded cubosome formulations that could be scaled to larger quantities [46]. The increased release of protein from cubosomes over shorter or equal timeframes in comparison to release from bulk LCP, Figure 1, is attributed to the fragmentation of the phase with increased surface area exposing water channels in the phase, reducing the time and distance required for diffusion of proteins into solution. Increased hydration of PHYT cubosomes results in larger water channel dimensions when compared to bulk cubic phases, Table 3. This may be a contributing factor in the observed faster release profiles from the cubosomes than from the bulk phase. As well as increased water channel dimensions, the cubosome formulation presents the cubic phase in a nanoparticle format, thus, shortening the distance required for incorporated proteins to diffuse out of the phase into solution. Previous analysis of the Pn3m mesophase of PHYT cubosomes have reported lattice parameters of 66 Å for blank cubosomes which are significantly lower than recorded parameters in Table 3 of between 110.3 – 115.6 Å.[27] Studies of PHYT dispersions stabilised with F127 have also reported lattice parameters of 71 Å.[79] However, the use of Tween 80 in the formulation of PHYT cubosomes has been reported to lead to increases in the lattice parameter

due to elevated hydration within the phase.[46] The addition of Tween 80 also was reported to cause phase transformations from Pn3m to Ia3d, due to interactions with the lipid bilayer as well as increased hydration within the phase which indicate that Tween 80 may be a useful stabilizer for the incorporation of large biomolecules.[46]

The zeta potential (ZP) values for all PHYT cubosome formulations were negative, Table 3, with the incorporation of ALDH increasing the negativity of the ZP value, whereas the incorporation of CYT C and GAPDH reduced the negativity of the ZP value. The calculated isoelectric points for incorporated proteins indicate a negative charge for ALDH in PBS solution and a positive charge for CYT C and GAPDH in PBS.[71],[70],[69] This indicates the isoelectric points of each protein has an impact on cubosome charge with positively charged proteins reducing the negative charge of the PHYT cubosomes whereas negatively charged proteins increase the negative charge of the cubosomes. Additionally, electrostatic surface mapping, Figure 4, indicates that all three proteins have a combination of positive and negative charges at their surface. This suggests that a percentage of the incorporated protein is present on or near the surface of the cubosome impacting the zeta potential of the particles. A similar outcome has been observed previously upon the introduction of FITC-Ova in PHYT cubosomes formulated with F127, a protein with negative surface charge in solution, which resulted in increasing the negative ZP value compared to blank cubosomes.[27]

The release of proteins from the PHYT bulk and cubosome formulations (or indeed the earlier discussed MO bulk cubic phase) did not reach 100% release for any incorporated protein. This is most likely due to the incorporated proteins closely matching or exceeding the dimensions of the aqueous channels within the phase and the electrostatic or hydrophobic interactions of the proteins with the lipids, thus trapping some of the incorporated protein within the tortuous network of the cubic phase. Incomplete release of proteins from LCP has been reported previously for large proteins such as ovalbumin (42.7 kDa) and conalbumin (75.8 kDa) as well as for smaller proteins such as myoglobin (15.3 kDa) and lysozyme (14.4 kDa).[24] A portion of incorporated protein may also be lost due to denaturation[24] or the presence of distorted areas of the cubic phase preventing release by diffusion.[80]

The activity assays, Figure 3, emphasize the propensity for encapsulation in the lipid cubic phase to prolong the biological activity of proteins. The cubosome dispersion is a low viscosity solution and therefore is more easily manipulated in an injectable formulation in comparison to the viscous bulk cubic phase. This is an attractive option for delivery of therapeutic proteins by injection to allow controlled release profiles and sustain activity beyond that observed for free proteins in solution. Site directed delivery using injection of protein loaded cubosomes compared to the current standard practice of intravenous delivery of therapeutic proteins could also increase concentration of protein at the site in comparison to systemic delivery.

5. Conclusion

A selection of proteins with varying aqueous solubilities, surface properties, stabilities and sizes were incorporated into and released from monoolein and phytantriol cubic phases. The ability of the lipid cubic system to incorporate large proteins while maintaining its structure attests to the flexibility of the system. The size and surface properties of the proteins incorporated were found to have a considerable impact on the release kinetics from the lipid cubic phase. The phytantriol cubic phase, both in bulk and cubosome formulations, was found to release active protein for prolonged periods of time in comparison to protein activity in solution. In some cases, enzyme activity was prolonged for up to three times longer upon encapsulation in the lipid cubic phase compared to the free protein in solution. The prolonged enzyme activity observed from proteins encapsulated in the lipid cubic phase is encouraging in relation to the development long-acting injectable protein formulations and the impact they can have on biotherapeutic expansion. Although the structure of the cubic phase system is well defined and stable in the presence of large soluble and insoluble proteins at low loadings, other factors such as lipid selection, formulation method, phase transitions, loading capacities and channel diameters will influence the release kinetics and specific activity of the encapsulated protein. The success of LCP as a protein delivery system is dependent on the physicochemical properties of the protein itself, including its size, isoelectric point, hydrophilicity, surface potential and inherent stability.

Funding Sources

This work was financially supported by Science Foundation Ireland, CÚRAM National University of Ireland, Galway and COOK Medical Ireland.

References

[1] M. Rajadhyaksha, T. Boyden, J. Liras, A. El-Kattan, J. Brodfuehrer, Current advances in delivery of biotherapeutics across the blood-brain barrier, Current drug discovery technologies 8(2) (2011) 87-101.

[2] D. Li, C.F. van Nostrum, E. Mastrobattista, T. Vermonden, W.E. Hennink, Nanogels for intracellular delivery of biotherapeutics, Journal of Controlled Release 259 (2017) 16-28.

[3] A.L. Daugherty, R.J. Mrsny, Formulation and delivery issues for monoclonal antibody therapeutics, Advanced drug delivery reviews 58(5-6) (2006) 686-706.

[4] A.C. Anselmo, Y. Gokarn, S. Mitragotri, Non-invasive delivery strategies for biologics, Nature Reviews Drug Discovery (2018).

[5] A. Angelova, B. Angelov, B. Papahadjopoulos-Sternberg, M. Ollivon, C. Bourgaux, Proteocubosomes: nanoporous vehicles with tertiary organized fluid interfaces, Langmuir 21(9) (2005) 4138-4143.

[6] T. Kaasgaard, C.J. Drummond, Ordered 2-D and 3-D nanostructured amphiphile self-assembly materials stable in excess solvent, Physical chemistry chemical physics 8(43) (2006) 4957-4975.

[7] H. Nakashima, K. Furukawa, Y. Kashimura, K. Torimitsu, Self-assembly of gold nanorods induced by intermolecular interactions of surface-anchored lipids, Langmuir 24(11) (2008) 5654-5658.

[8] J.C. Shah, Y. Sadhale, D.M. Chilukuri, Cubic phase gels as drug delivery systems, Advanced drug delivery reviews 47(2-3) (2001) 229-250.

[9] S.T. Hyde, Identification of lyotropic liquid crystalline mesophases, Handbook of applied surface and colloid chemistry 2 (2001) 299-332.

[10] L.B. Lopes, D.A. Ferreira, D. de Paula, M.T.J. Garcia, J.A. Thomazini, M.C. Fantini, M.V.L. Bentley, Reverse hexagonal phase nanodispersion of monoolein and oleic acid for topical delivery of peptides: in vitro and in vivo skin penetration of cyclosporin A, Pharmaceutical research 23(6) (2006) 1332-1342.

[11] Y. Chen, P. Ma, S. Gui, Cubic and hexagonal liquid crystals as drug delivery systems, BioMed research international 2014 (2014).

[12] S.B. Rizwan, B.J. Boyd, T. Rades, S. Hook, Bicontinuous cubic liquid crystals as sustained delivery systems for peptides and proteins, Expert opinion on drug delivery 7(10) (2010) 1133-1144.

[13] E.M. Landau, J.P. Rosenbusch, Lipidic cubic phases: a novel concept for the crystallization of membrane proteins, Proceedings of the National Academy of Sciences 93(25) (1996) 14532-14535.
[14] M. Caffrey, Crystallizing membrane proteins for structure determination: use of lipidic mesophases, Annual review of biophysics 38 (2009) 29-51.
[15] A. Angelova, B. Angelov, R. Mutafchieva, S. Lesieur, P. Couvreur, Self-assembled multicompartment liquid crystalline lipid carriers for protein, peptide, and nucleic acid drug delivery, Accounts of chemical research 44(2) (2011) 147-156.
[16] B. Angelov, A. Angelova, U. Vainio, V.M. Garamus, S. Lesieur, R. Willumeit, P. Couvreur, Long-living intermediates during a lamellar to a diamond-cubic lipid phase transition: a small-angle X-ray scattering investigation, Langmuir 25(6) (2009) 3734-3742.
[17] S. Leslie, S. Puvvada, B. Ratna, A. Rudolph, Encapsulation of hemoglobin in a bicontinuous cubic phase lipid, Biochimica et Biophysica Acta (BBA)-Biomembranes 1285(2) (1996) 246-254.
[18] E. Nazaruk, M. Szlęzak, E. Górecka, R. Bilewicz, Y.M. Osornio, P. Uebelhart, E.M. Landau, Design and assembly of pH-sensitive lipidic cubic phase matrices for drug release, Langmuir 30(5) (2014) 1383-1390.
[19] M. Dully, C. Brasnett, A. Djeghader, A. Seddon, J. Neilan, D. Murray, J. Butler, T. Soulimane, S.P. Hudson, Modulating the release of pharmaceuticals from lipid cubic phases using a lipase inhibitor, Journal of Colloid and Interface Science (2020).
[20] C.J. Drummond, C. Fong, Surfactant self-assembly objects as novel drug delivery vehicles, Current opinion in colloid & interface science 4(6) (1999) 449-456.
[21] M.L. Lynch, A. Ofori-Boateng, A. Hippe, K. Kochvar, P.T. Spicer, Enhanced loading of water-soluble actives into bicontinuous cubic phase liquid crystals using cationic surfactants, Journal of colloid and interface science 260(2) (2003) 404-413.
[22] K. Lindell, J. Engblom, S. Engström, M. Jonströmer, A. Carlsson, Influence of a charged phospholipid on the release pattern of timolol maleate from cubic liquid crystalline phases, The Colloid Science of Lipids, Springer1998, pp. 111-118.
[23] J. Clogston, G. Craciun, D. Hart, M. Caffrey, Controlling release from the lipidic cubic phase by selective alkylation, Journal of controlled release 102(2) (2005) 441-461.

[24] J. Clogston, M. Caffrey, Controlling release from the lipidic cubic phase. Amino acids, peptides, proteins and nucleic acids, Journal of controlled release 107(1) (2005) 97-111.
[25] B. Ericsson, K. Larsson, K. Fontell, A cubic protein-monoolein-water phase, Biochimica et Biophysica Acta (BBA)-Biomembranes 729(1) (1983) 23-27.
[26] S. Rizwan, T. Hanley, B.J. Boyd, T. Rades, S. Hook, Liquid crystalline systems of phytantriol and glyceryl monooleate containing a hydrophilic protein: characterisation, swelling and release kinetics, Journal of pharmaceutical sciences 98(11) (2009) 4191-4204.
[27] S. Rizwan, D. Assmus, A. Boehnke, T. Hanley, B. Boyd, T. Rades, S. Hook, Preparation of phytantriol cubosomes by solvent precursor dilution for the delivery of protein vaccines, European journal of pharmaceutics and biopharmaceutics 79(1) (2011) 15-22.
[28] A. Misiūnas, Z. Talaikytė, G. Niaura, V. Razumas, T. Nylander, Thermomyces lanuginosus lipase in the liquid-crystalline phases of aqueous phytantriol: X-ray diffraction and vibrational spectroscopic studies, Biophysical chemistry 134(3) (2008) 144-156.
[29] B. Angelov, A. Angelova, S.K. Filippov, M. Drechsler, P. Stepanek, S. Lesieur, Multicompartment lipid cubic nanoparticles with high protein upload: Millisecond dynamics of formation, ACS nano 8(5) (2014) 5216-5226.
[30] T. Nylander, C. Mattisson, V. Razumas, Y. Miezis, B. Håkansson, A study of entrapped enzyme stability and substrate diffusion in a monoglyceride-based cubic liquid crystalline phase, Colloids and Surfaces A: Physicochemical and Engineering Aspects 114 (1996) 311-320.
[31] H. Chung, M. Caffrey, The curvature elastic-energy function of the lipid–water cubic mesophase, Nature 368(6468) (1994) 224-226.
[32] E. Nazaruk, A. Majkowska-Pilip, R. Bilewicz, Lipidic Cubic-Phase Nanoparticles—Cubosomes for Efficient Drug Delivery to Cancer Cells, ChemPlusChem 82(4) (2017) 570-575.
[33] T. Ishida, H. Kiwada, Alteration of tumor microenvironment for improved delivery and intratumor distribution of nanocarriers, Biological and Pharmaceutical Bulletin 36(5) (2013) 692-697.
[34] H. Maeda, Tumor-selective delivery of macromolecular drugs via the EPR effect: background and future prospects, Bioconjugate chemistry 21(5) (2010) 797-802.

[35] R.P. Patil, D.D. Pawara, C.S. Gudewar, A.R. Tekade, Nanostructured cubosomes in an in situ nasal gel system: an alternative approach for the controlled delivery of donepezil HCl to brain, Journal of liposome research 29(3) (2019) 264-273.
[36] M. Said, A.A. Aboelwafa, A.H. Elshafeey, I. Elsayed, Central composite optimization of ocular mucoadhesive cubosomes for enhanced bioavailability and controlled delivery of voriconazole, Journal of Drug Delivery Science and Technology 61 (2021) 102075.
[37] N. Oh, J.-H. Park, Endocytosis and exocytosis of nanoparticles in mammalian cells, International journal of nanomedicine 9(Suppl 1) (2014) 51.
[38] A. Tan, L. Hong, J.D. Du, B.J. Boyd, Self-assembled nanostructured lipid systems: is there a link between structure and cytotoxicity?, Advanced Science 6(3) (2019) 1801223.
[39] J.A. Prange, S. Aleandri, M. Komisarski, A. Luciani, A. Käch, C.-D. Schuh, A.M. Hall, R. Mezzenga, O. Devuyst, E.M. Landau, Overcoming endocytosis deficiency by cubosome nanocarriers, ACS Applied Bio Materials 2(6) (2019) 2490-2499.
[40] M.M. Mehanna, R. Sarieddine, J.K. Alwattar, R. Chouaib, H. Gali-Muhtasib, Anticancer Activity of Thymoquinone Cubic Phase Nanoparticles Against Human Breast Cancer: Formulation, Cytotoxicity and Subcellular Localization, International Journal of Nanomedicine 15 (2020) 9557.
[41] E. Jabłonowska, D. Matyszewska, E. Nazaruk, M. Godlewska, D. Gaweł, R. Bilewicz, Lipid membranes exposed to dispersions of phytantriol and monoolein cubosomes: Langmuir monolayer and HeLa cell membrane studies, Biochimica et Biophysica Acta (BBA)-General Subjects 1865(1) (2021) 129738.
[42] T. Landh, Phase behavior in the system pine needle oil monoglycerides-Poloxamer 407-water at 20. degree, The journal of physical chemistry 98(34) (1994) 8453-8467.
[43] D. Ledward, Effects of pressure on protein structure, International Journal of High Pressure Research 19(1-6) (2000) 1-10.
[44] N. Jonckheere, N. Skrypek, I. Van Seuningen, Mucins and pancreatic cancer, Cancers 2(4) (2010) 1794-1812.
[45] P.T. Spicer, K.L. Hayden, M.L. Lynch, A. Ofori-Boateng, J.L. Burns, Novel process for producing cubic liquid crystalline nanoparticles (cubosomes), Langmuir 17(19) (2001) 5748-5756.

[46] H. Azhari, M. Strauss, S. Hook, B.J. Boyd, S.B. Rizwan, Stabilising cubosomes with Tween 80 as a step towards targeting lipid nanocarriers to the blood–brain barrier, European Journal of Pharmaceutics and Biopharmaceutics 104 (2016) 148-155.
[47] A. Yaghmur, H. Mu, Recent advances in drug delivery applications of cubosomes, hexosomes, and solid lipid nanoparticles, Acta Pharmaceutica Sinica B 11(4) (2021) 871-885.
[48] H. Liu, Y. Wang, Q. Wang, Z. Li, Y. Zhou, Y. Zhang, S. Li, Protein-bearing cubosomes prepared by liquid precursor dilution: inner ear delivery and pharmacokinetic study following intratympanic administration, Journal of biomedical nanotechnology 9(10) (2013) 1784-1793.
[49] A. Angelova, M. Ollivon, A. Campitelli, C. Bourgaux, Lipid cubic phases as stable nanochannel network structures for protein biochip development: X-ray diffraction study, Langmuir 19(17) (2003) 6928-6935.
[50] M. Rakotoarisoa, B. Angelov, S. Espinoza, K. Khakurel, T. Bizien, A. Angelova, Cubic liquid crystalline nanostructures involving catalase and curcumin: BioSAXS study and catalase peroxidatic function after cubosomal nanoparticle treatment of differentiated SH-SY5Y cells, Molecules 24(17) (2019) 3058.
[51] J. Barauskas, A. Misiunas, T. Gunnarsson, F. Tiberg, M. Johnsson, “Sponge” nanoparticle dispersions in aqueous mixtures of diglycerol monooleate, glycerol dioleate, and polysorbate 80, Langmuir 22(14) (2006) 6328-6334.
[52] B. Ericsson, P. Eriksson, J. Löfroth, S. Engström, Cubic phases as delivery systems for peptide drugs, ACS Publications1991.
[53] Y. Sadhale, J.C. Shah, Biological activity of insulin in GMO gels and the effect of agitation, International journal of pharmaceutics 191(1) (1999) 65-74.
[54] S. Engström, T.P. Nordén, H. Nyquist, Cubic phases for studies of drug partition into lipid bilayers, European journal of pharmaceutical sciences 8(4) (1999) 243-254.
[55] C.-M. Chang, R. Bodmeier, Low viscosity monoglyceride-based drug delivery systems transforming into a highly viscous cubic phase, International journal of pharmaceutics 173(1-2) (1998) 51-60.
[56] C. Mattos, D. Ringe, Proteins in organic solvents, Current opinion in structural biology 11(6) (2001) 761-764.
[57] H. Wu, J. Li, Q. Zhang, X. Yan, L. Guo, X. Gao, M. Qiu, X. Jiang, R. Lai, H. Chen, A novel small Odorranalectin-bearing cubosomes: Preparation, brain delivery

and pharmacodynamic study on amyloid-β25–35-treated rats following intranasal administration, European journal of pharmaceutics and biopharmaceutics 80(2) (2012) 368-378.
[58] T.K. Kwon, J.C. Kim, In vitro skin permeation of monoolein nanoparticles containing hydroxypropyl β-cyclodextrin/minoxidil complex, International journal of pharmaceutics 392(1-2) (2010) 268-273.
[59] N.M. Morsi, G.A. Abdelbary, M.A. Ahmed, Silver sulfadiazine based cubosome hydrogels for topical treatment of burns: development and in vitro/in vivo characterization, European journal of pharmaceutics and biopharmaceutics 86(2) (2014) 178-189.
[56] S. Biffi, L. Andolfi, C. Caltagirone, C. Garrovo, A.M. Falchi, V. Lippolis, A. Lorenzon, P. Macor, V. Meli, M. Monduzzi, Cubosomes for in vivo fluorescence lifetime imaging, Nanotechnology 28(5) (2016) 055102.
[57] W. Leesajakul, M. Nakano, A. Taniguchi, T. Handa, Interaction of cubosomes with plasma components resulting in the destabilization of cubosomes in plasma, Colloids and Surfaces B: Biointerfaces 34(4) (2004) 253-258.
[58] J. Bode, J. Kuntsche, S. Funari, H. Bunjes, Interaction of dispersed cubic phases with blood components, International journal of pharmaceutics 448(1) (2013) 87-95.
[59] T. Soulimane, G. Buse, G.P. Bourenkov, H.D. Bartunik, R. Huber, M.E. Than, Structure and mechanism of the aberrant ba3-cytochrome c oxidase from Thermus thermophilus, The EMBO journal 19(8) (2000) 1766-1776.
[60] K. Hayes, M. Noor, A. Djeghader, P. Armshaw, T. Pembroke, S. Tofail, T. Soulimane, The quaternary structure of Thermus thermophilus aldehyde dehydrogenase is stabilized by an evolutionary distinct C-terminal arm extension, Scientific reports 8(1) (2018) 1-14.
[61] M.C. Fisher, J. Bosch, Z. Yin, D.A. Stead, J. Walker, L. Selway, A.J. Brown, L.A. Walker, N.A. Gow, J.E. Stajich, Proteomic and phenotypic profiling of the amphibian pathogen Batrachochytrium dendrobatidis shows that genotype is linked to virulence, Molecular ecology 18(3) (2009) 415-429.
[62] H. Qiu, M. Caffrey, The phase diagram of the monoolein/water system: metastability and equilibrium aspects, Biomaterials 21(3) (2000) 223-234.
[63] J. Barauskas, T. Landh, Phase behavior of the phytantriol/water system, Langmuir 19(23) (2003) 9562-9565.

[64] N.H. Kim, M.S. Jeong, S.Y. Choi, J.H. Kang, Peroxidase activity of cytochrome c, Bull Korean Chem Soc 25(1889) (2004) 92.
[65] M. Szlezak, D. Nieciecka, A. Joniec, M. Pękała, E. Gorecka, M.I. Emo, M.J. Stébé, P. Krysiński, R. Bilewicz, Monoolein cubic phase gels and cubosomes doped with magnetic nanoparticles–hybrid materials for controlled drug release, ACS applied materials & interfaces 9(3) (2017) 2796-2805.
[66] Z. Karami, M. Hamidi, Cubosomes: remarkable drug delivery potential, Drug discovery today 21(5) (2016) 789-801.
[67] P. Wadsten-Hindrichsen, J. Bender, J. Unga, S. Engström, Aqueous self-assembly of phytantriol in ternary systems: effect of monoolein, distearoylphosphatidylglycerol and three water-miscible solvents, Journal of colloid and interface science 315(2) (2007) 701-713.
[68] J. Kyte, R.F. Doolittle, A simple method for displaying the hydropathic character of a protein, Journal of molecular biology 157(1) (1982) 105-132.
[69] E. Gasteiger, C. Hoogland, A. Gattiker, M.R. Wilkins, R.D. Appel, A. Bairoch, Protein identification and analysis tools on the ExPASy server, The proteomics protocols handbook, Springer2005, pp. 571-607.
[70] B. Bjellqvist, B. Basse, E. Olsen, J.E. Celis, Reference points for comparisons of two-dimensional maps of proteins from different human cell types defined in a pH scale where isoelectric points correlate with polypeptide compositions, Electrophoresis 15(1) (1994) 529-539.
[71] B. Bjellqvist, G.J. Hughes, C. Pasquali, N. Paquet, F. Ravier, J.C. Sanchez, S. Frutiger, D. Hochstrasser, The focusing positions of polypeptides in immobilized pH gradients can be predicted from their amino acid sequences, Electrophoresis 14(1) (1993) 1023-1031.
[72] N.A. Baker, D. Sept, S. Joseph, M.J. Holst, J.A. McCammon, Electrostatics of nanosystems: application to microtubules and the ribosome, Proceedings of the National Academy of Sciences 98(18) (2001) 10037-10041.
[73] T.J. Dolinsky, J.E. Nielsen, J.A. McCammon, N.A. Baker, PDB2PQR: an automated pipeline for the setup of Poisson–Boltzmann electrostatics calculations, Nucleic acids research 32(suppl_2) (2004) W665-W667.
[74] E. Nazaruk, P. Miszta, S. Filipek, E. Górecka, E.M. Landau, R. Bilewicz, Lyotropic cubic phases for drug delivery: Diffusion and sustained release from the

mesophase evaluated by electrochemical methods, Langmuir 31(46) (2015) 12753-12761.
[75] P. Astolfi, E. Giorgini, F.C. Adamo, F. Vita, S. Logrippo, O. Francescangeli, M. Pisani, Effects of a cationic surfactant incorporation in phytantriol bulk cubic phases and dispersions loaded with the anticancer drug 5-fluorouracil, Journal of Molecular Liquids 286 (2019) 110954.
[76] R. Brown, E. Madrid, R. Castaing, J.M. Stone, A.M. Squires, K.J. Edler, K. Takashina, F. Marken, Free-standing phytantriol Q (224) cubic-phase films: Resistivity monitoring and switching, ChemElectroChem 4(5) (2017) 1172-1180.
[77] S. Hyde, S. Andersson, A cubic structure consisting of a lipid bilayer forming an infinite periodic minimum surface of the gyroid type in the glycerolmonooleat-water system, Zeitschrift für Kristallographie-Crystalline Materials 168(1-4) (1984) 213-220.
[78] B. Tenchov, R. Koynova, G. Rapp, Accelerated formation of cubic phases in phosphatidylethanolamine dispersions, Biophysical journal 75(2) (1998) 853-866.
[79] S.J. Fraser, X. Mulet, A. Hawley, F. Separovic, A. Polyzos, Controlling nanostructure and lattice parameter of the inverse bicontinuous cubic phases in functionalised phytantriol dispersions, Journal of colloid and interface science 408 (2013) 117-124.
[80] K. Moebus, J. Siepmann, R. Bodmeier, Cubic phase-forming dry powders for controlled drug delivery on mucosal surfaces, Journal of controlled release 157(2) (2012) 206-215.

CRediT authorship contribution statement

Sally Ryan: Conceptualization, Methodology, Validation, Formal analysis, Investigation, Writing - original draft, Visualization, Funding acquisition, Data curation. **Kim Shortall:** Methodology, Writing - review & editing, **Michele Dully:** Methodology. **Ahmed Djehedar:** Supervision. **David Murray:** Supervision, Resources. **James Butler:** Supervision, Resources. **John Neilan:** Supervision, Resources. **Tewfik Soulimane:** Conceptualization, Resources, Writing - review & editing, Supervision, Project administration, Funding acquisition. **Sarah P. Hudson:** Conceptualization, Resources, Writing - review & editing, Supervision, Project administration, Funding acquisition.

Declaration of interests

☒ The authors declare that they have no known competing financial interests or personal relationships that could have appeared to influence the work reported in this paper.

☐The authors declare the following financial interests/personal relationships which may be considered as potential competing interests:

Graphical abstract

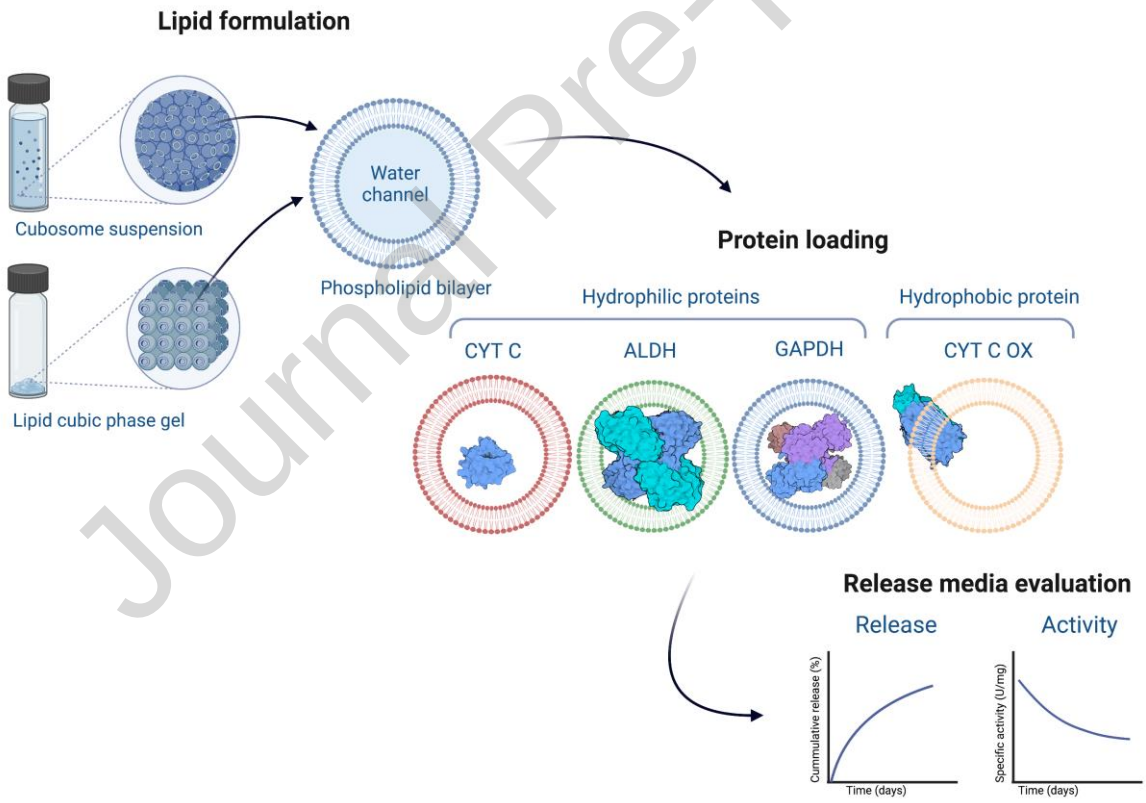

Highlights

- Bulk and dispersed lipid cubic phases (LCP) can be injected parenterally
- Bulk and dispersed LCP can incorporate large proteins
- Size and surface properties of proteins incorporated impact on release kinetics
- Enzyme activity can last 3 times longer in LCPs compared to free protein in solution